

# Growth and field emission properties of vertically-aligned ZnO nanowire array on biaxially textured Ni-W substrate by thermal evaporation

Deepak Chhikara, K. M. K. Srivatsa\*, M. Senthil Kumar, Preetam Singh, Sourav Das, O. S. Panwar

*Physics of Energy Harvesting Division, Council of Scientific & Industrial Research (CSIR) - National Physical Laboratory, Dr. K.S. Krishnan Marg, New Delhi-110012, India*

\*Corresponding author. Tel: (+91)11 45721075; E-mail: [kmk\\_srivatsa@mail.nplindia.org](mailto:kmk_srivatsa@mail.nplindia.org)

Received: 05 March 2015, Revised: 10 July 2015 and Accepted: 19 July 2015

## ABSTRACT

Vertically well aligned and highly dense ZnO nanowires (NWs) have been grown on biaxially textured Ni substrates by a simple thermal evaporation technique over a large area without using any catalyst. The grown ZnO NWs have crystallized in wurtzite hexagonal structure and have grown along [0001] direction. It is also observed that the degree of vertical alignment of NWs increases with increasing growth temperature. An intense photoluminescence peak at 383 nm with a negligible deep band emission revealed the good crystalline quality of ZnO NWs. Field emission properties of the grown NWs have been examined and a field enhancement factor of 1573 has been obtained, indicating the suitability of grown nanowires for field emission applications. Copyright © 2015 VBRI Press.

**Keywords:** ZnO Nanowires; thermal evaporation; Raman spectrum; field emission.

## Introduction

One dimensional (1D) Zinc Oxide (ZnO) nanostructure semiconductor material is intensely studied for the last two decades and maintains its space for research due to its numerous promising applications in various devices viz. solar cells, photo-catalysts, chemical sensors, thermoelectric and piezoelectric devices because of the direct wide band gap (3.37 eV) and high exciton binding energy (60 meV) of ZnO at room temperature [1]. Several researchers have been putting efforts to synthesize various ZnO nanostructures following different techniques for variety of applications [2-12]. In particular, well-aligned or micro-patterned arrays of 1D ZnO nanostructures are highly desirable for promising device applications. It has been demonstrated that ZnO nanowire arrays can emit ultraviolet laser at room temperature [13], while a large-area, hexagonal patterned ZnO nanorod/nanowire arrays are expected to find potential applications as nano-optoelectronic devices, nano-sensor arrays [14] and solar cells [15]. The properties of ZnO nanowires are direction dependence and for the piezoelectric and field emission device fabrication, a vertical array of ZnO NWs is preferred [16]. However, there are many issues related to the growth of desired vertically aligned NWs. Controlled morphology and seed-free growth of ordered ZnO nanorod structure is very difficult on many substrates because of lattice mismatch [17]. In catalyst assisted growth the nano-wires

end up with catalyst particle which is not suitable for field emission application. Also, the electrical and thermal conductivity of the substrate play a crucial role in fabricating thermoelectric, piezoelectric and field emission nano-devices based on vertically-aligned ZnO NWs [18], in respect of good electrical communication and thermal dissipation during device operation. The other issues are related to the growth of high aspect ratio, degree of vertical alignment and the density of nanostructures. The growth process and related parameters play the main role to meet all these requirements.

While the semiconducting substrates can be doped to increase the electrical conductivity, a direct growth of vertically-aligned ZnO NWs on metallic substrates is preferred for improved electrical and thermal conduction, which in turn could improve the device performance by using substrate as one of the electrodes [18]. Many researchers have employed different metals and their alloys as a substrate viz. FeCrAl, Fe-Co-Ni, Copper and Nickel foil, for the growth of aligned ZnO 1D structures by various deposition techniques such as solution method, hydro-thermal technique, vapor transport technique, thermal evaporation, and chemical-bath depositions [18-27]. Among them, thermal evaporation is an easy, environmental friendly and low-cost process. Ni substrate has the advantage of good corrosion resistance and thermal stability compared to other metal substrates. Only Zaleszczyk *et al.* has reported the growth of ZnO nanorods

on nickel substrate using the thermal evaporation technique, but no alignment was observed [22]. In this work, we have made an attempt to grow the vertically aligned nanowires on Ni substrate and discuss the obtained results. These results suggest that the current approach enables to achieve vertically well aligned NWs while meeting the major requirements for field emission application.

## Experimental

### Materials synthesis

For this study, Zn powder (99.99%, Merck, Germany), Ar, O<sub>2</sub> (99.999%, BOC, India), gases, and (200) oriented biaxially Ni-5at% W (Ni-W) substrate procured from the manufacturer M/s Evico GmbH, Germany have been used. Growth of ZnO NWs was carried out in a horizontal quartz-tube reactor at a growth temperature in the range of 600–700 °C. The cleaned substrates were placed over pure zinc powder taken in an alumina boat and the set-up was later loaded in to the centre of the quartz reactor. Initially, the quartz reactor was flushed with 2000 sccm of N<sub>2</sub> gas for 20 minutes to clean the growth environment. Then, the furnace temperature was ramped to a designated temperature under the N<sub>2</sub> gas flow of 1200 sccm and is kept constant for all the growth runs. After reaching the growth temperature, O<sub>2</sub> gas flow of 5 sccm was added through a mass flow controller. The growth time was fixed as 10 minutes for all the experiments. At the end, the quartz furnace was switched off and was allowed to cool down naturally to the room temperature under the same gas flow condition. The samples were then taken out for further characterizations. White colour deposition was observed over the whole substrate.

### Characterizations

For The samples were characterized with scanning electron microscopy (SEM, ZEISS EVO MA 10) for the morphology and their crystalline properties were investigated by x-ray diffraction (XRD, D8-Advance, M/s Bruker) with CuK $\alpha$ 1 radiation. Photoluminescence (PL, F-900, Edinburg Instruments, UK) and Raman spectroscopy (Renishaw Invia Raman Microscope) were also measured at room temperature using a xenon lamp (at 325nm) and an Ar<sup>+</sup> laser (514 nm) as the excitation sources, respectively. Field Emission (FE) properties of ZnO NWs have been investigated at room temperature by a parallel plate geometry using a high voltage source meter (Keithley model 2410) in a vacuum environment of 2.5 $\times$ 10<sup>-7</sup> mbar pressure. The distance between the anode and the top of ZnO NWs (cathode) was fixed by using a 150  $\mu$ m thick spacer. An ITO coated glass substrate was used as the anode. A 5 mm diameter circular area of the ZnO NW array was used for the field emission study.

## Results and discussion

The  $\theta$ -2 $\theta$  X-ray scans of Ni-W alloy substrate and the ZnO nanostructures grown at various temperatures are shown in **Fig. 1**. The Ni-W substrate showed a single orientation along (002) direction (JCPDS No. 04-0850). ZnO NWs showed a dominant peaks of [002] planes along with other peaks of low intensity. The XRD peaks could be indexed to

the wurtzite hexagonal structure of ZnO as confirmed by the JCPDS card No. 65-3411. A sharp, intense (002) peak indicates that the ZnO nanostructures have c-axis orientation and are likely grown normal to the substrate. In XRD spectra of ZnO NWs at 700 °C, a low intensity peak related to NiO with (111) orientation (JCPDS card No. 47-1049) has also been observed indicating the formation of a thin NiO layer at the interface.

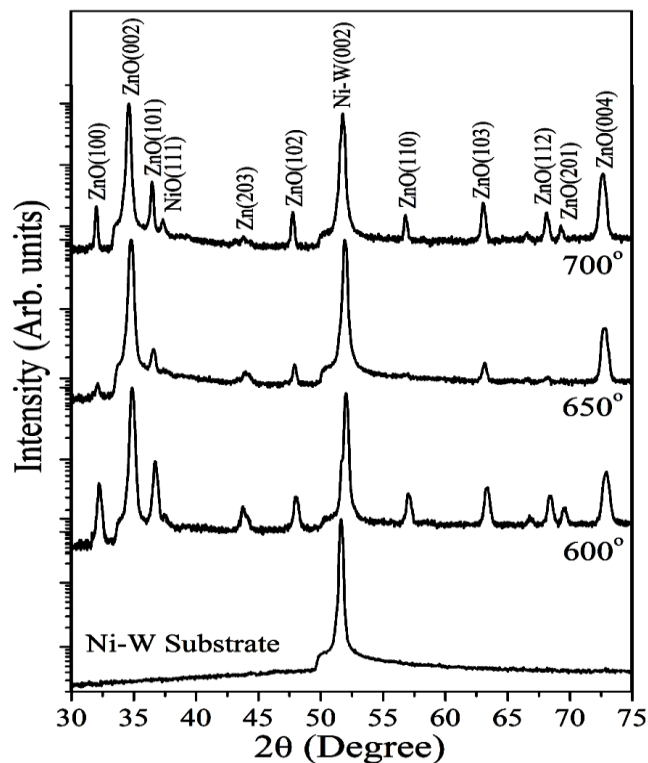


**Fig. 1.** XRD spectra of Ni-W substrate and ZnO NWs grown at various temperatures.

Surface morphology of the Ni-W substrate and the grown ZnO nanostructures are presented in **Fig. 2**. The SEM image of Ni-W substrate shows large area grains of an average size of 30–40 nm as in **Fig. 2(a)**. At 600 °C, randomly aligned growth of ZnO NWs has been observed as seen in **Fig. 2 (b)**. Some secondary structure growth has also occurred at few places that may probably happen during the cooling period of the reactor. From the SEM micrographs it is evident that the alignment of micro-wires improved with temperature and at 700 °C well vertical alignment normal to the substrate has been observed, **Fig. 2(c-f)**. Also, the growth of ZnO NWs occurred in a large scale on Ni-W substrates with a high density and large grains of about 30–40 nm. The comparable grain sizes before and after NW growth indicates that the ZnO growth mimics the textured surface of the Ni-W substrate. Boundary lines between the NWs grown on two adjacent grains could be clearly observed confirming that the grain boundaries do not promote the ZnO NW growth. Thus employing the biaxially textured substrate in place of normal substrate is advantageous to increase the density of NW due to reduced grain boundary areas. The inset of **Fig. 2(f)** clearly shows the formation of hexagonal facet of ZnO NWs at the end indicating that the NWs grow along the (0002) direction. Also, the NW tips are free of any catalyst,

which make them suitable for field emission applications. EDS spectrum gives the elemental information in atomic percentage and that of the vertically aligned ZnO NWs is presented in **Fig. 2(g)**. The EDS spectrum confirmed that the NWs are made up of zinc and oxygen atoms of near stoichiometry. A very less at % of Ni was also seen in the spectrum that arises from the Ni substrate and/or NiO interface layer.

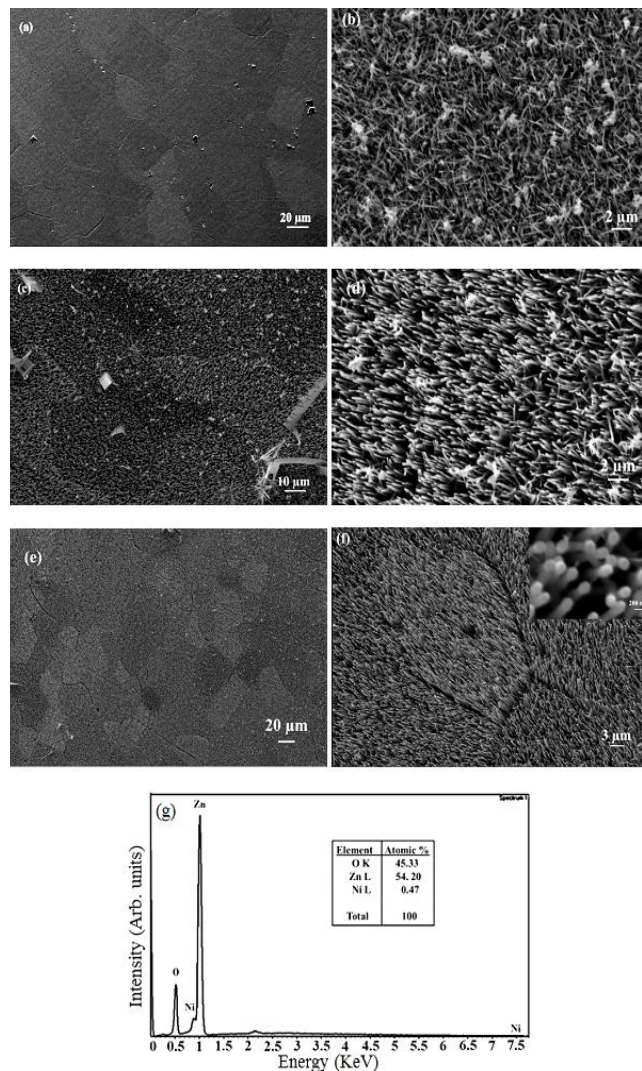


**Fig. 2.** SEM surface morphology of (a) Ni-W substrate, and ZnO nanowires grown at (b) 600 °C, (c & d) 650 °C and (e & f) 700 °C. Inset of (f) gives the magnified image of the nanowires, (g) EDS spectrum of the ZnO NWs grown at 700 °C.

The crystalline properties of the grown ZnO NWs were further characterized by TEM analysis. **Fig. 3(a)** shows the TEM image of a single NW of 80~100 nm in diameter with uniform thickness and the diameter shrinks to 20 nm at the tip of the NW. The HRTEM and SAED show the single crystalline nature of the grown NW as in **Fig. 3(b)** and **3(c)**, respectively. The spacing between adjacent lattice planes of about 0.26 nm corresponds to adjacent plane distance of ZnO (002) indicating that the NW grows along c-axis over Ni-W substrate as indicated by the high diffraction intensity of (002) plane in the XRD. The NWs with sharp tip is favorable for field emission applications.

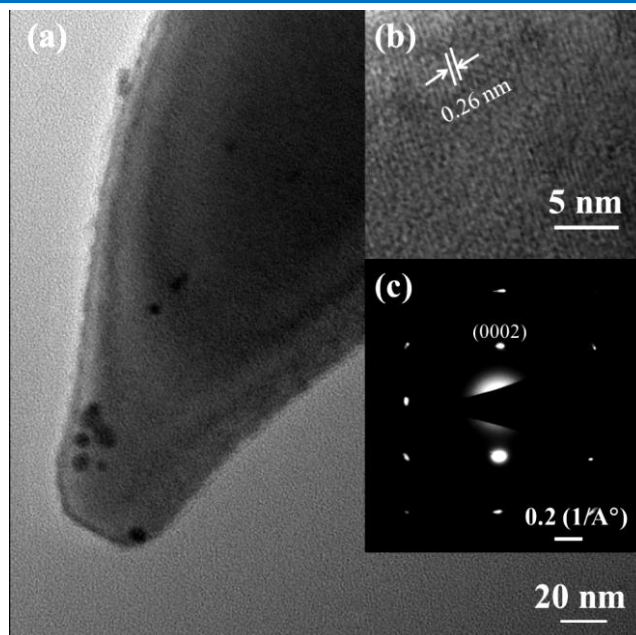


**Fig. 3.** HRTEM images of ZnO nanowire grown at 700 °C: (a) Low and (b) High magnifications, and (c) SAED pattern.

The growth of NWs without any catalyst at their tip also hints a vapor-solid (V-S) based growth mechanism. The proposed growth mechanism for obtained vertically well aligned NWs is schematically represented in **Fig. 4**. Initially, at elevated temperature above 600 °C in presence of oxygen flow it is likely that the Ni surface is oxidized and a thin NiO layer is formed with (111) preferential orientation which leads to ZnO 1D nanostructure normal to the substrate.

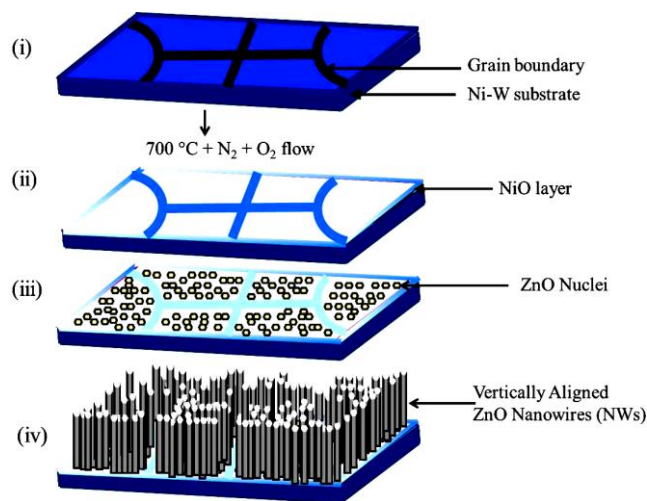


**Fig. 4 (i-iv).** Schematic diagram of the proposed growth mechanism for vertically aligned ZnO nanowires at 700 °C on the surface of Ni-W substrate.

Because of the similarity between the hexagonal and the cubic crystal forms, good lattice matching conditions may be expected if the cubic lattice edge is  $\sqrt{2}$  times the hexagonal lattice constant (a-axis) and the c-axis is grown perpendicular to the (111) plane [28]. The large lattice mismatch of about 22% between NiO and ZnO could lead to formation of localized ZnO (0001) nuclei and promote

the vertical growth of ZnO NWs. The improved degree of vertical alignment of NWs at 700 °C may be attributed to the better crystallinity of NiO layer. Using carbo-thermal evaporation Zaleszczyk *et al.* have reported randomly oriented ZnO nanorod growth on nickel substrate with a Ni<sub>0.79</sub>Zn<sub>0.21</sub>O polycrystalline interface layer, where the growth was carried out at a very high temperature of 930 °C resulting strong reaction between ZnO and Ni at the interface [22].

The structural properties of the ZnO NWs were also investigated by Raman scattering measurement at room temperature in the range 200-800 cm<sup>-1</sup> and the typical spectrum is presented in **Fig. 5(a)**. The Raman spectrum consisted of several bands that correspond to Raman-active phonon modes of wurtzite ZnO that belongs to C46v space group. Among the following optical modes of crystalline ZnO viz. A1+2B1+E1+2E2, the A1, E1 and E2 modes are Raman active. B1 mode is silent and A1 and E1 modes are also infrared active [29]. The Raman active E2 mode is non-polar and it gives two frequencies i.e. E2 (high) corresponding to oxygen atoms and E2 (low) corresponding to Zinc. A1 and E1 are polar phonon modes, therefore split into two: longitudinal (LO) and transverse (TO) optical components [30]. A sharp and dominant peak was observed at 438 cm<sup>-1</sup> corresponding to the Raman active E2 (high) vibration mode, which is the characteristic of hexagonal wurtzite phase of ZnO. Two weak peaks at 331 cm<sup>-1</sup> and 381 cm<sup>-1</sup> were observed and they referred to E2 (high) – E2 (low) (multi phonon) and A1 (TO) modes, respectively. The higher intensity of Raman active E2 mode indicates that the grown ZnO NWs possess well-crystallized wurtzite hexagonal phase. A typical room temperature PL spectrum of the vertically aligned ZnO NW array is given in **Fig. 5(b)**.

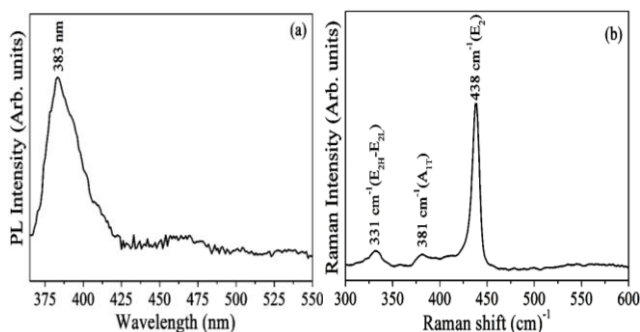


**Fig. 5.** Room temperature (a) Raman and (b) PL spectra of the vertically aligned ZnO NWs array grown at 700 °C.

The NWs exhibit a strong UV emission at 383 nm (3.24 eV), with a negligible deep band emission. The UV emission peak belongs to the near band edge emission (NBE) of ZnO, which occurs due to the free exciton transition from the localized level below the conduction band to the valence band, i.e. the recombination of free excitons through an exciton-exciton collision [31]. A high UV to visible emission ratio demonstrates the good crystalline quality of the grown ZnO NW arrays.

Field emission measurements were carried out on the best aligned ZnO NW array grown at 700 °C. The following Fowler-Nordheim (F-N) equation has been be

used to study the field emission properties of the ZnO aligned grown NWs,

$$J = \frac{A\beta^2 E^2}{\phi} \exp\left(\frac{-B\phi^{3/2}}{\beta E}\right)$$

where, J is the current density, A & B are constants with the values of  $1.56 \times 10^{-10} \text{ AV}^{-2} \text{ eV}$  and  $6.83 \times 10^3 \text{ V (eV)}^{-3/2} \mu\text{m}^{-1}$ , E is the applied field ( $E=V/d$ , where V and d are the applied voltage and the distance between the anode and the sample (cathode)),  $\phi$  is the work function, which is taken as 5.3 eV for ZnO from the literature [32] and  $\beta$  is the field-enhancement factor that gives the ability of the emitters to enhance the local electric field.  $\beta$  can be calculated from  $-B\phi^{3/2}/S$ , where S belongs to the slope of F-N plot. Inset of **Fig. 6** shows the plot of  $\ln(J/E^2)$  vs.  $1/E$  (the F-N Plot).

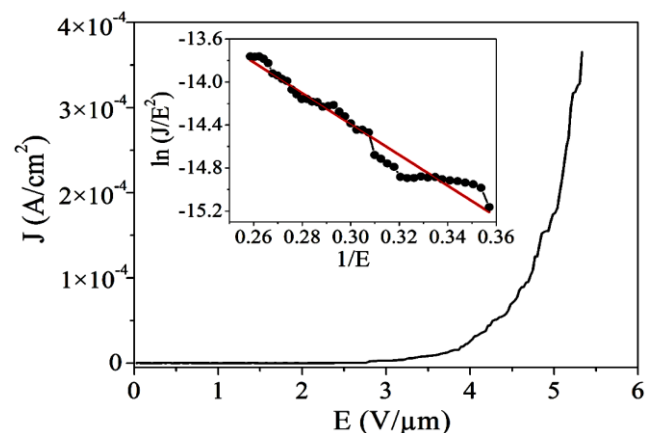


**Fig. 6.** Field emission properties of vertically aligned ZnO 1D NWs (J-E plot). Plot shows the turn-on electric field of 2.7 V/μm at a current density of 1 μA/cm<sup>2</sup>. The inset shows the corresponding Fowler-Nordheim (F-N) plot.

The measured current density J (A/cm<sup>2</sup>) as a function of applied electric field E (V/μm) is shown in **Fig. 6**. The turn-on electric field is obtained as 2.73 V/μm at a current density of 1 μA/cm<sup>2</sup>.

In this study, the  $\beta$  value is calculated from the linear fitting of the slope of F-N plot to be 1573. The value of  $\beta$  is dependent upon the alignment, sharpness and the density of the grown structure over the substrate. In our case, the ZnO NWs are of high density with good structural uniformity. Also, the diameter of the NWs reduced towards the tip favoring the field emission that can enhance the  $\beta$  value and increase the gap between NWs in the array that can diminish the screening effect. The metal substrate also plays an important role in achieving good electrical contact to the NWs. In literature, a wide range of  $\beta$  values have been reported depending upon the ZnO nanostructure morphology. Kuo *et al.* have obtained a  $\beta$  value of 642 from the vertical ZnO NW array deposited on Si substrate by chemical vapor deposition [32]. Liu *et al.* reported a  $\beta$  value of 2350 for the vertically aligned ZnO nanoneedle array on Fe-Co-Ni substrate grown by solution approach [19]. Thus, the obtained  $\beta$  value of 1573 in this report is comparable with the literature and is good enough for various field emission applications.

## Conclusion

We have successfully grown vertically well aligned ZnO NWs biaxially textured on Ni-W substrate over a large area using the simple thermal evaporation technique. It is found that the ZnO NWs growth occurs uniformly over the large grains of the textured substrate separated by the grain boundaries. The degree of alignment is found to depend on the growth temperature and improves with increasing growth temperature. XRD, SEM, TEM and Raman studies confirm the single crystalline nature of the grown NWs. The well-aligned ZnO NWs with sharp tip offers a good field enhancement factor of 1573, which is useful to fabricate efficient field emission devices.

## Acknowledgements

The authors gratefully acknowledge the Council of Scientific and Industrial Research (CSIR) for the funding through the research grant No. OLP-120132. The authors also gratefully acknowledge the help of Dr. D. Haranath, Dr. R.P. Pant, Dr. B.P. Singh, Mr. Dinesh Singh, Mr. Ravikant Tripathi, and Mr. Jay Tawale for PL, XRD, Raman, TEM, Field Emission and SEM measurements, respectively.

## Author contributions

Conceived the plan: DC, KMKS, MSK; Performed the experiments: DC, SD; Data analysis: DC, KMKS, MKS, PS, SD, OSP; Wrote the paper: DC, KMKS, MSK, PS. Authors have no competing financial interests.

## Reference

- Meyyappan, M.; Sunkara, MK. *Inorganic Nanowires: Application, Properties and Characterization*. Boca Raton, FL: CRC Press, 2010.
- Tian, ZR.; Voigt, JA.; Liu, J.; McKenzie, B.; JM.; Rodriguez, MA.; Konishi, H.; Xu, H. *Nat. Mater.* **2003**, *2*, 821. DOI: [10.1038/nmat1014](https://doi.org/10.1038/nmat1014)
- Fan, HJ.; Knez, M.; Scholz, R.; Nielsch, K.; Pippel, E.; Hesse, D.; Zacharias, M.; Gosele, U. *Nat. Mater.* **2006**, *5*, 627. DOI: [10.1038/nmat1673](https://doi.org/10.1038/nmat1673)
- Agarwal, DC.; Chauhan, RS.; Avasthi, DK.; Sulania, I.; Kabiraj, D.; Thakur, P.; Chae, KH.; Chawla, A.; R Chandra, Ogale, SB.; Pellegrini, G.; Mazzoldi, P. *Journal of Physics D: Applied Physics*, **2009**, *42*, 035310. DOI: [10.1088/0022-3727/42/3/035310](https://doi.org/10.1088/0022-3727/42/3/035310)
- Zeng, H.; Duan, G.; Li, Y.; Yang, S.; Xu, X.; Cai, W. *Advanced Functional Materials*, **2010**, *20*, 561. DOI: [10.1002/adfm.200901884](https://doi.org/10.1002/adfm.200901884)
- Mishra, YK.; Chakravadhanula, VSK.; Hrkac, V.; Jebiril, S.; Agarwal, DC.; Mohapatra, S.; Avasthi, DK.; Kienle, L.; Adelung, R. *J. Appl. Phys.* **2012**, *112*, 064308. DOI: [10.1063/1.4752469](https://doi.org/10.1063/1.4752469)
- Mishra, YK.; Kaps, S.; Schuchardt, A.; Paulowicz, I.; Jin, X.; Gedamu, D.; Freitag, S.; Claus, M.; Wille, S.; Kovalev, A.; Gorb, SN.; Adelung, R. *Part. Part. Syst. Charact.*, **2013**, *30*, 775. DOI: [10.1002/ppsc.201300197](https://doi.org/10.1002/ppsc.201300197)
- Mishra, YK.; Kaps, S.; Schuchardt, A.; Paulowicz, I.; Jin, X.; Gedamu, D.; Wille, S.; Lupan, O.; Adelung, R. *Kona Powder and Particle Journal.*, **2014**, *31*, 92. DOI: [10.14356/kona.2014015](https://doi.org/10.14356/kona.2014015)
- Reimer, T.; Paulowicz, I.; Röder, R.; Kaps, S.; Lupan, O.; Chemnitz, S.; Benecke, W.; Ronning, C.; Adelung, R.; Mishra, YK. *ACS Appl. Mater. Interfaces*, **2014**, *6* (10), 7806. DOI: [10.1021/am5010877](https://doi.org/10.1021/am5010877)
- Baranwala, V.; Zahrab, A.; Singh, PK.; Pandeya, AC. *J. Alloys Compd.*, **2015**, *646*, 238. DOI: [10.1016/j.jallcom.2015.06.007](https://doi.org/10.1016/j.jallcom.2015.06.007)
- Srivastava, S.; Srivastava, AK.; Singh, P.; Baranwala, V.; Kripal, R.; Lee, J-H.; Pandeya, AC. *J. Alloys Compd.*, **2015**, *644*, 597. DOI: [10.1016/j.jallcom.2015.04.220](https://doi.org/10.1016/j.jallcom.2015.04.220)
- Mishra, YK.; Modi, G.; Cretu, V.; Postica, V.; Lupan, O.; Reimer, T.; Paulowicz, I.; Hrkac, V.; Benecke, W.; Kienle, L.; Adelung, R. *ACS Appl. Mater. Interfaces*, **2015**, *7*, 14303. DOI: [10.1021/acsami.5b02816](https://doi.org/10.1021/acsami.5b02816)

- Huang, MH.; Mao, S.; Feick, H.; Yan, H.; Wu, Y.; Kind, H.; Weber, E.; Russo, R.; Yang, P. *Science.*, **2001**, *292*, 1897. DOI: [10.1126/science.1060367](https://doi.org/10.1126/science.1060367)
- Wang, X.; Summers, CJ.; Wang, ZL. *Nano Lett.*, **2004**, *4*, 423. DOI: [10.1021/nl035102c](https://doi.org/10.1021/nl035102c)
- Law, M.; Greene, LE.; Johnson, JC.; Saykally, R.; Yang, P. *Nature Mater.*, **2005**, *4*, 455. DOI: [10.1038/nmat1387](https://doi.org/10.1038/nmat1387)
- Wang, ZL.; Song, JH. *Science.*, **2006**, *312*, 242. DOI: [10.1126/science.1124005](https://doi.org/10.1126/science.1124005)
- Ibupoto, ZH.; Khun, K.; Eriksson, M.; AlSalhi, M.; Atif, M.; Ansari, A.; Willander, M. *Materials.*, **2013**, *6*, 3584. DOI: [10.3390/ma6083584](https://doi.org/10.3390/ma6083584)
- Ngo-Duc, T.; Singh, K.; Meyyappan, M.; Oye, MM. *Nanotechnology.*, **2012**, *23*, 194015. DOI: [10.1088/0957-4484/23/19/194015](https://doi.org/10.1088/0957-4484/23/19/194015)
- Liu, J.; Huang, X.; Li, Y.; Ji, X.; Li, Z.; He, X.; Sun, F. *J. Phys. Chem. C.*, **2007**, *111*, 4990. DOI: [10.1021/jp067782o](https://doi.org/10.1021/jp067782o)
- Zhang, S.; Shen, Y.; Fang, H.; Xu, S.; Song, J.; Wang, ZL. *J. Mater. Chem.*, **2010**, *20*, 10606. DOI: [10.1039/C0JM02915G](https://doi.org/10.1039/C0JM02915G)
- Ngo-Duc, TT.; Gacusan, J.; Kobayashi, NP.; Sanghadasa, M.; Meyyappan, M.; Oye, MM. *Appl. Phys. Lett.*, **2013**, *102*, 083105. DOI: [10.1063/1.4793758](https://doi.org/10.1063/1.4793758)
- Zaleszczyk, W.; Fronc, K.; Przedziecka, E.; Janik, E.; Presz, A.; Czapkiewicz, M.; Wrobel, J.; Paszkowicz, W.; Klopotoski, L.; Karczewski, G.; Wojtowicz, T. *Acta Phys. Polonica A.*, **2008**, *114*, 1451. DOI: [2008AcPPA.114.1451Z](https://doi.org/10.1063/1.2200472)
- Umar, A.; Hahn, YB. *Appl. Phys. Lett.*, **2006**, *88*, 173120. DOI: [10.1063/1.2200472](https://doi.org/10.1063/1.2200472)
- Zainelabdin, A.; Zaman, S.; Amin, G.; Nur O.; Willander, M. *Cryst. Growth Des.*, **2010**, *10*, 3250. DOI: [10.1021/cg100390x](https://doi.org/10.1021/cg100390x)
- Yun, Y.; Tailing, G.; Yadong, J. *J. Semicond.*, **2012**, *33*, 043003. DOI: [10.1088/1674-4926/33/4/043003](https://doi.org/10.1088/1674-4926/33/4/043003)
- Abbasi, MA.; Ibupoto, ZH.; Khan, Y.; Khan, A.; Nur, O.; Willander, M. *J. Sensors.*, **2013**, 382726. DOI: [10.1155/2013/382726](https://doi.org/10.1155/2013/382726)
- Liu, J.; Li, Y.; Huang, X. 2nd IEEE International Nanoelectronics Conference (INEC), **2008**, 53.
- Echresh, A.; Abbasi, MA.; Shoushtari, MZ.; Farbod, M.; Nur, O.; Willander, M. *Semicond. Sci. Technol.*, **2014**, *29*, 115009. DOI: [10.1088/0268-1242/29/11/115009](https://doi.org/10.1088/0268-1242/29/11/115009)
- Cheng, HM.; Hsu, HC.; Tseng, YK.; Lin, LJ.; Hsieh, WF. *J. Phys. Chem. B.*, **2005**, *109*, 8749. DOI: [10.1021/jp0442908](https://doi.org/10.1021/jp0442908)
- Sieber, B.; Liu, H.; Piret, G.; Laureyns, J.; Roussel, P.; Gelloz, B.; Szunerites, S.; Boukherroub, R. *J. Phys. Chem. C.*, **2009**, *113*, 13643. DOI: [10.1021/jp903504w](https://doi.org/10.1021/jp903504w)
- Cho, S.; Ma, J.; Kim, Y.; Sun, Y.; Wong GKL.; Ketterson, JB. *Appl. Phys. Lett.*, **1999**, *75*, 2761. DOI: [10.1063/1.125141](https://doi.org/10.1063/1.125141)
- Kuo, SY.; Lin, HL. *Nano. Res. Lett.*, **2014**, *9*, 70. DOI: [10.1186/1556-276X-9-70](https://doi.org/10.1186/1556-276X-9-70)

## Advanced Materials Letters

Copyright © VBRI Press AB, Sweden  
[www.vbripress.com](http://www.vbripress.com)

Publish your article in this journal

Advanced Materials Letters is an official international journal of International Association of Advanced Materials (IAAM, [www.iaamonline.org](http://www.iaamonline.org)) published by VBRI Press AB, Sweden monthly. The journal is intended to provide top-quality peer-review articles in the fascinating field of materials science and technology particularly in the area of structure, synthesis and processing, characterisation, advanced-state properties, and application of materials. All published articles are indexed in various databases and are available download for free. The manuscript management system is completely electronic and has fast and fair peer-review process. The journal includes review article, research article, notes, letter to editor and short communications.

